



A quick measurement method for determining the incidence angle modifier of flat plate solar collectors using spectroradiometer

Article

Accepted Version

Creative Commons: Attribution-Noncommercial-No Derivative Works 4.0

Tian, Z., Deng, J., Zhang, S., Yao, R. and Shao, L. (2020) A quick measurement method for determining the incidence angle modifier of flat plate solar collectors using spectroradiometer. *Solar Energy*, 201. pp. 746-750. ISSN 0038-092X doi: <https://doi.org/10.1016/j.solener.2020.03.059> Available at <http://centaur.reading.ac.uk/89540/>

It is advisable to refer to the publisher's version if you intend to cite from the work. See [Guidance on citing](#).

To link to this article DOI: <http://dx.doi.org/10.1016/j.solener.2020.03.059>

Publisher: Elsevier

All outputs in CentAUR are protected by Intellectual Property Rights law,

including copyright law. Copyright and IPR is retained by the creators or other copyright holders. Terms and conditions for use of this material are defined in the [End User Agreement](#).

www.reading.ac.uk/centaur

CentAUR

Central Archive at the University of Reading

Reading's research outputs online

1 *A technical note (short communication) for Solar Energy*

2

3 **A quick measurement method for determining the incidence angle**
4 **modifier of flat plate solar collectors using spectroradiometer**

5

6 Zhiyong Tian ^a, Jie Deng ^{b,*}, Shicong Zhang ^c, Runming Yao ^b, Li Shao ^b

7 ^a Department of Civil and Environmental Engineering, Norwegian University of
8 Science and Technology, Trondheim, Norway

9 ^b School of The Built Environment, University of Reading, Whiteknights, Reading,
10 Berkshire, RG6 6DF, UK

11 ^c China Academy of Building Research, Beijing 100013, China

12

13

14 * Corresponding author:

15 E-mail address: deng-jie2@163.com, j.deng@reading.ac.uk (J. Deng)

16

17

18 **A quick measurement method for determining the incidence angle**
19 **modifier of flat plate solar collectors using spectroradiometer**

20

21 **Abstract**

22 In real engineering of solar thermal applications, it needs considerable effort to
23 determine the incidence angle modifier (IAM) of flat plate solar collectors, according
24 to the test standards (BS EN ISO 9806, 2017; ASHRAE 93-2010, 2014). And the
25 available method in the test standards is usually inapplicable to measure thermal
26 performance of installed solar collectors with dust deposition effect in service. A quick
27 measurement method is therefore presented to identify the IAM of flat plate solar
28 collectors with less effort using a spectroradiometer. The quick method developed was
29 validated with optical tests of a solar panel under the conditions of different incidence
30 angles. It is inferred that the method not only helps to determine the IAM of flat plate
31 solar collectors quickly without needing to run the collectors by energy power input,
32 but also provides a pathway for assessing dust deposition effect on the thermal
33 performance of installed flat plate solar collectors in service, as well as for determining
34 the optical property attenuation of solar collectors in the long-term running.

35

36 *Keywords:* Flat plate solar collector; Incidence angle modifier (IAM);
37 Spectroradiometer; Reflectance spectrum; Irradiance spectrum

38

39

40 **List of symbols**

Nomenclature	
A_a	collector aperture area or transparent cover area, m^2
A_g	collector gross area, m^2
b_0	constant of the incidence angle modifier of flat plate solar collectors, dimensionless
F_R	heat removal factor of a solar collector, dimensionless
G_g	global solar irradiance on tilted solar collector surface, W/m^2
$Irr_{50^\circ}(\lambda)$	solar spectral irradiance with a tilted angle of 50° at λ nm wavelength, $W/(m^2 nm)$
$Irr_{90^\circ}(\lambda)$	solar spectral irradiance with a tilted angle of 90° at λ nm wavelength, $W/(m^2 nm)$
$K_{\theta b}(\theta)$	incidence angle modifier of solar beam radiation for a solar collector with an incidence angle of θ degree, dimensionless
Q_u	useful heat gain of solar collector, W/m^2
T_{amb}	ambient temperature, $^\circ C$
T_{fi}	collector inlet temperature, $^\circ C$
T_m^*	$=(T_{fi} - T_{amb})/G_g$, normalised temperature difference, $(m^2 \text{ }^\circ C)/W$
U_L	collector total heat loss coefficient, $W/(m^2 \text{ }^\circ C)$
<i>Greek symbols</i>	
η_a	collector thermal efficiency based on collector aperture area, dimensionless
η_g	collector thermal efficiency based on collector gross area, dimensionless
θ	incidence angle of solar beam radiation on a solar collector, $^\circ$
λ	wavelength, nm
ρ_{tot}	total reflectance at the top of a solar collector, dimensionless
$\rho_{tot,c}(\lambda)$	corrected total reflectance at λ nm wavelength, dimensionless
$\rho_{tot,m}(\lambda)$	measured total reflectance at λ nm wavelength with the vertical reference plane, dimensionless
$(\tau\alpha)_{en}$	effective transmittance-absorptance product of a solar collector at normal incidence (or optical efficiency), dimensionless
$(\tau\alpha)_\theta$	effective transmittance-absorptance product of a solar collector at an incidence angle of θ degree, dimensionless
<i>Abbreviations</i>	
<i>IAM</i>	incidence angle modifier

42 **1 Introduction**

43 Dynamic or transient thermal characteristics of flat plate solar collectors in naturally
44 variable meteorological conditions are widely concerned in low-temperature solar
45 thermal applications (Rojas et al., 2008; Deng et al., 2015a; Deng et al., 2016; Deng et
46 al., 2017; Tian et al., 2018; Aleksiejuk et al., 2018). The incidence angle modifier (IAM)
47 of the flat plate solar collectors plays an important role in the collector dynamic thermal
48 performance due to diurnal motion of the sun. It is therefore indispensable to determine
49 the collector IAM in assessing and predicting collector dynamic thermal performance
50 in real engineering. Following the solar collector test standards (BS EN ISO 9806, 2017;
51 ASHRAE 93-2010, 2014), however, it usually takes considerable efforts to obtain the
52 IAM of flat plate solar collectors through thermal performance tests recommended. The
53 collector thermal performance at fixed incidence angles (e.g. 0°, 30°, 45°, 60°) is
54 needed to test in order to get the IAMs. The solar collectors need to be run under specific
55 incidence angle conditions over a period of time by power energy input and the test
56 requirement is relatively rigorous in the steady-state. Particularly, determination of the
57 IAM of solar collectors with variable geometries is more complicated because there are
58 more than one direction of dependence for the IAM (Sallaberry et al., 2015; Hertel et
59 al., 2015). The present study aims to introduce a quick measurement method for
60 identifying the collector IAM using a spectroradiometer. The collector IAM can be
61 obtained through executing a couple of quick optical test sequences without running
62 the solar collectors by energy power input, meaning that less effort is taken to obtain
63 the IAM compared to the thermal performance test method recommended in the

64 existing test standards. More than that, the quick method is expected to assess dust
 65 deposition effect on the thermal performance of installed flat plate solar collectors in
 66 service on-site of solar fields, as well as to determine optical performance attenuation
 67 of the solar collectors in the long-term running in terms of optical tests. Table 1 gives
 68 a comparison between the available methods in the test standards and the presented
 69 method, which indicates the advantages of the latter.

70

71 Table 1. Comparison between the method available in the test standards and the
 72 presented method

Comparison of test conditions	Thermal performance test method available in the test standards	The presented method using spectroradiometer
Running solar collectors by energy input	Need thermal power	No need
Test conditions of incidence angles	Fixed incidence angles (e.g. 0°, 30°, 45°, 60°) which are restricted	Flexible incidence angles can be chosen as long as it covers a wide range from 0° to 60°.
Test duration	Considerable efforts with restricted conditions (tends to cover several sunny days)	Less effort (usually can be completed on one sunny day)
Applicability in determining optical property of installed solar collectors with surface dust deposition	Unable to determine dust deposition effect without intervention of normal operating of the solar collectors	Applicable to determine dust deposition effect and optical property attenuation of on-site solar collectors

73

74 **2 Fundamentals of the measurement method**

75

76 **2.1 Thermal performance test method available in the test standards for**
77 **determining the collector IAM**

78 Usually, the collector thermal efficiency (η_a) based on collector aperture area (A_a) is
79 defined as (Duffie and Beckman, 2013):

80
$$\eta_a = \frac{Q_u}{A_a G_g} = \frac{A_g}{A_a} \eta_g \quad (1)$$

81
82

83 Concerning the collector thermal efficiency curve correlating η_g (or η_a) with the
84 normalised temperature difference ($T_m^* = (T_{fi} - T_{amb})/G_g$), a simple linear model in
85 equation (2) is commonly used to describe the collector steady-state thermal
86 performance (Duffie and Beckman, 2013; BS EN ISO 9806, 2017; ASHRAE 93-2010,
87 2014).

88

89
$$\eta_g = \frac{A_a}{A_g} \cdot \left[F_R (\tau\alpha)_{en} \cdot K_{\theta b}(\theta) - F_R U_L \frac{(T_{fi} - T_{amb})}{G_g} \right] \quad (2)$$

90

91 where $K_{\theta b}(\theta)$ – the collector IAM of solar beam radiation is described as (BS EN
92 ISO 9806, 2017):

93
$$K_{\theta b}(\theta) = 1 - b_0 \cdot \left(\frac{1}{\cos\theta} - 1 \right) \quad (3)$$

94

95 where θ is the incidence angle of solar beam radiation on the collector surface, °; b_0
96 is a constant of the IAM of the flat plate solar collector, dimensionless.

97

98 In the solar collector test standards (BS EN ISO 9806, 2017; ASHRAE 93-2010, 2014),

99 the thermal performance test method is recommended in determining the collector IAM
100 by testing the collector thermal efficiency at different incidence angles.

101

102 **2.2 Fundamental of determining the collector IAM using spectroradiometer**

103 Essentially, the optical efficiency $((\tau\alpha)_\theta)$ of the flat plate solar collectors can be
104 separated from the collector thermal efficiency curve in Equation (2), as shown in
105 Equation (4).

106

$$107 \quad (\tau\alpha)_\theta = (\tau\alpha)_{en} \cdot [1 - b_0 \cdot (1/\cos\theta - 1)] \quad (4)$$

108 where the optical efficiency $(\tau\alpha)_\theta$ represents the transmittance-absorptance product
109 of the collector at an incidence angle of θ (Duffie and Beckman, 2013).

110

111 The total reflectance (ρ_{tot}) of the solar collectors is calculated in Equation (5), since
112 the sum of the transmittance-absorptance product and the total reflectance equals one
113 in terms of energy conservation. As the total reflectance (ρ_{tot}) at the top of the collector
114 surface in equation (5) can be measured directly using a spectrometer with a white
115 reflectance standard, it is convenient to obtain the transmittance-absorptance products
116 $((\tau\alpha)_\theta)$ of a flat plate solar collector at different incidence angles by measuring the total
117 reflectance. Then the IAM is readily identified through linear fitting of $(\tau\alpha)_\theta$ versus
118 the incidence angle (θ) . It is reckoned as a quick measurement method to identify the
119 collector IAM, since there is no need to run the collectors for thermal performance tests

120 by energy power input and it can be completed on one sunny day.

$$121 \quad \rho_{tot} = 1 - (\tau\alpha)_\theta \quad (5)$$

122

123 **3 Method validation with real tests and merit explanation**

124 **3.1 Test facilities and procedures of implementing the quick method**

125 A Black-Comet-SR concave grating miniature spectrometer (CXR-SR, StellarNet Inc.,
126 USA) was used to measure the total reflectance at the top of a flat plate solar panel at
127 different incidence angles, in order to determine the constant (b_0) of the IAM in
128 Equation (4). The miniature spectrometer has a spectroradiometer mode by fitting the
129 fiber-optic cable with a cosine receptor (180° field of view), which allows measuring
130 solar spectral irradiance in a range of wavelengths from 350 to 1000 nm. The fiber-
131 optic tip of the spectrometer with a white reflectance standard RS50 is shown in Figure
132 1(a). A solar panel with a tilted angle of 40° shown in Figure 1(b) was used for optical
133 tests under a clear sky. Manufacturing information of the panel was not available and
134 disregarded, as the [quick method did not require detailed information of the optical](#)
135 [system and its components.](#) There was a technical problem of directly measuring the
136 total reflectance in Equation (5), because the white reference standard had to be tilted
137 at the same angle as the solar panel (40° in the case), while the fiber-optic tip pointing
138 at the white reference standard would shade the reference standard on a sunny day. To
139 avoid the technical problem, a vertical reference plane (90° tilted angle) was taken in
140 the tests of the total reflectance at different incidence angles. In the meanwhile, solar

141 irradiance spectra at the tilted angles of 90°, 50° were recorded instantaneously with the
142 fiber-optic tip upwards fitted with the cosine receptor. Thus, the original total
143 reflectance measured based on the vertical reference plane can be corrected by
144 conversions of solar spectral irradiances, as given in Equation (6).

145

$$146 \quad \rho_{tot,c}(\lambda) = \rho_{tot,m}(\lambda) \cdot Irr_{50^\circ}(\lambda) / Irr_{90^\circ}(\lambda) \quad (6)$$

147

148 where $\rho_{tot,c}(\lambda)$ is the corrected total reflectance at λ nm wavelength. $\rho_{tot,m}(\lambda)$ is
149 the measured total reflectance at λ nm wavelength with the vertical reference plane.
150 $Irr_{50^\circ}(\lambda)$ and $Irr_{90^\circ}(\lambda)$ denotes the solar spectral irradiance at λ nm wavelength
151 with tilted angles of 50° and 90°, respectively.

152

153 The average reflectance ($\rho_{tot,ave}$) at a specific incidence angle can be calculated as

$$154 \quad \rho_{tot,ave} = \sum_{350}^{1000} \rho_{tot,m}(\lambda) \cdot Irr_{50^\circ}(\lambda) / \sum_{350}^{1000} Irr_{90^\circ}(\lambda) \quad (7)$$

155



156

157 (a)



(b)

158 Figure 1 Testing facilities (a) fiber-optic tip of the spectrometer and reflectance standard

159 RS50; (b) solar panel in test

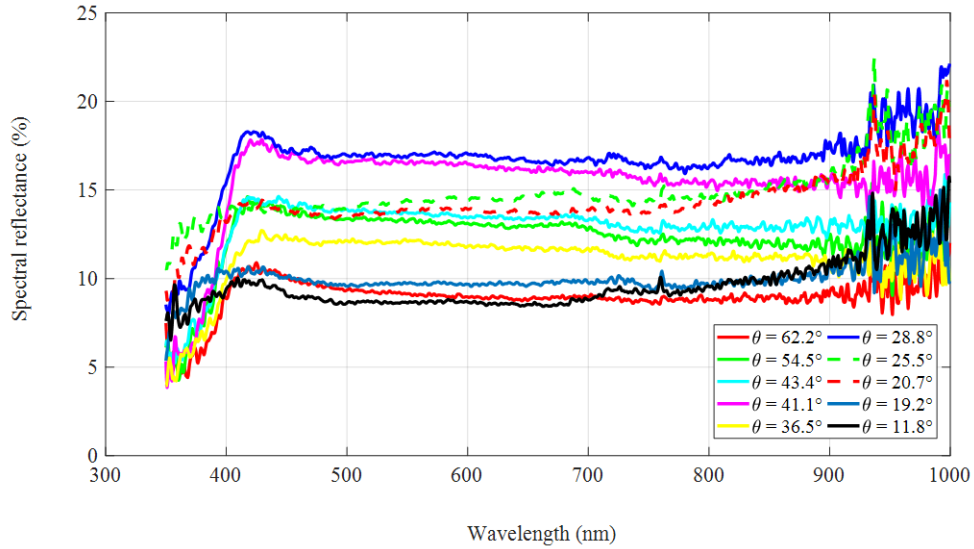
160

161 A set of test sequences was executed with the solar panel at different incidence angles
162 to determine the IAM. In a test condition of a specific incidence angle, the total
163 reflectance spectrum of the solar panel with the vertical reference plane, solar spectral
164 irradiance at both tilted angles of 50° and 90° were measured in a quick succession. A
165 ruler was used to measure the shadow length of a fixed-length rod perpendicular to the
166 surface of the panel, giving rise to the incidence angle which was the arctangent value
167 of the quotient of rod shadow length divided by rod length.

168

169 **3.2 Reflectance spectra of the solar panel at different incidence angles**

170 Through a group of optical tests with the solar panel at different incidence angles, the
171 measured total reflectance spectrum of the solar panel with the vertical reference plane,
172 the measured solar spectral irradiance at tilted angles of 50° and 90° were obtained on
173 a sunny day. Figure 2 shows the measured reflectance spectrum of the tested solar panel
174 with fiber-optic tip pointing in the normal direction of the solar panel and to a vertical
175 reference plane, while Figure 3 gives the corrected reflectance spectra at different
176 incidence angles using equation (6), combining the measured solar spectral irradiance
177 at tilted angles of 50° and 90° .



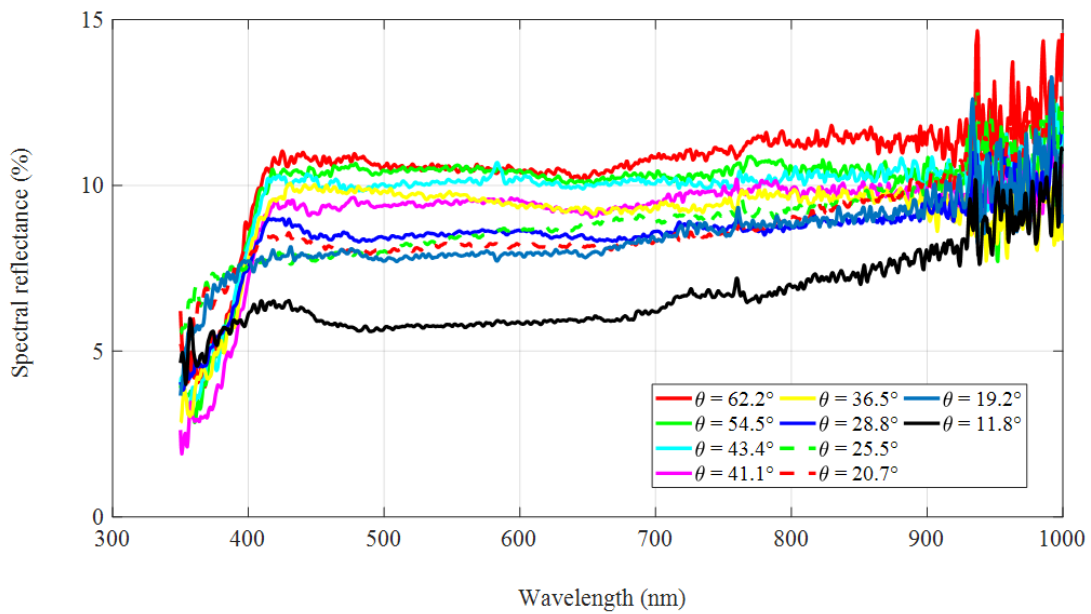
178

179 Figure 2 Measured reflectance spectrum of the tested solar panel with fiber-optic tip

180 pointing in the normal direction of the solar panel and to a vertical reference plane

181

182



183

184 Figure 3 Corrected reflectance spectra at different incidence angles for the solar panel

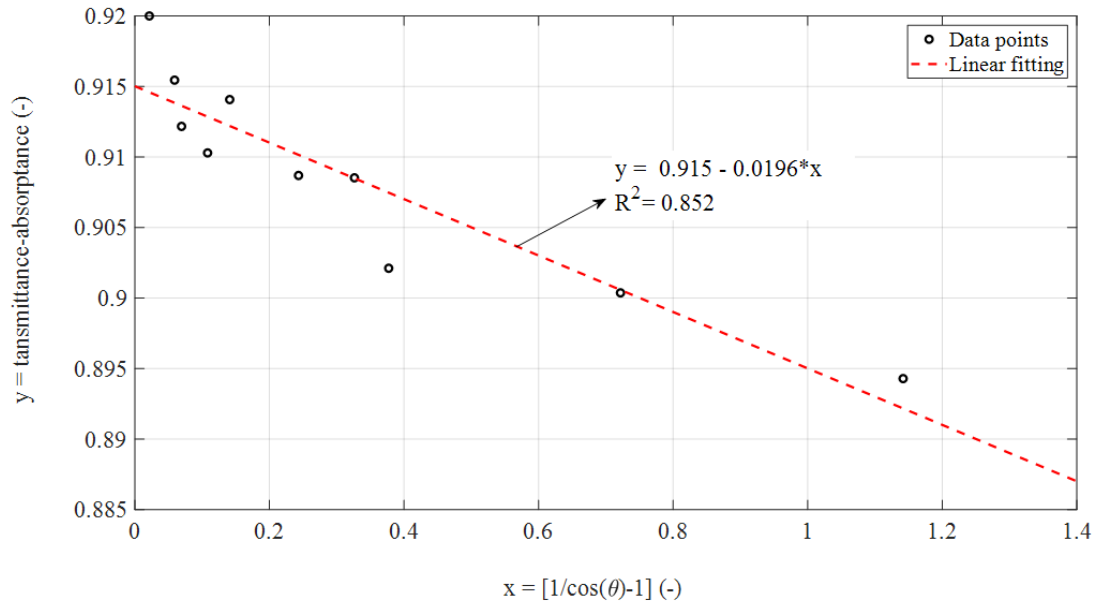
185 tested

186

187 3.3 Linear fitting of the IAM (incidence angle modifier)

188 Based on the corrected reflectance spectra at different incidence angles for the solar
189 panel (see Figure 3), the total reflectance at the top of the solar panel surface was
190 calculated in equation (7). Then the transmittance-absorptance products $(\tau\alpha)_\theta$ at
191 different incidence angles (θ) were obtained in equation (5). Figure 4 gives the linear
192 fitting results of the transmittance-absorptance product $(\tau\alpha)_\theta$ versus $[1/\cos\theta - 1]$,
193 in terms of the relations between each other described in equation (3). The coefficient
194 of determination (R^2) in the fitting was 0.852, indicating a high correlation of $(\tau\alpha)_\theta$
195 versus $[1/\cos\theta - 1]$. The root mean square error of the fitting was 0.31%. Fitting
196 coefficients and their standard uncertainties in the linear fitting model were $(\tau\alpha)_{en} =$
197 0.915 ± 0.0015 and $-b_0 \cdot (\tau\alpha)_{en} = 0.0196 \pm 0.0032$, respectively. Thus, the
198 coefficients $(\tau\alpha)_{en}$ and $b_0 \cdot (\tau\alpha)_{en}$ and their standard uncertainties result in $b_0 =$
199 $\frac{0.0196}{0.915} = 0.0214 \pm 0.0035$. At here, the constant b_0 of the IAM was lower than
200 presented in the literature (Tesfamichael and Wäckelgård, 2000; Tian et al., 2017; Tian
201 et al., 2018), mainly due to the fact that a solar photovoltaic panel was used for the tests.
202 For flat plate solar thermal collectors, the constant b_0 tends to be in the range of 0.1–
203 0.3 according to the literature. Nonetheless, it confirms that applying the optical tests
204 by using a spectroradiometer is feasible to determine the IAM of flat plate solar
205 collectors.

206



207

208 Figure 4 Linear fitting of transmittance-absorptance product $(\tau\alpha)_\theta$ versus $[1/\cos\theta -$
 209 $1]$ ($x = b_0 \cdot (1/\cos\theta - 1)$, $y = (\tau\alpha)_\theta$)

210

211 3.4 Merits of the presented quick measurement method

212 As the presented method decouples the IAM from measuring the collector thermal
 213 efficiency and directly applies tests of collector optical efficiency, it helps to save lots
 214 of effort comparing with the available method in the test standards (see Table 1). More
 215 than that, the method is applicable to determine the collector optical efficiency in some
 216 other scenarios in real engineering. Specifically, dust and ash in the air might be
 217 deposited on the installed flat plate solar collectors in service. The effect of dirt can
 218 degrade the transmittance of transparent covers of flat plate solar collectors to some
 219 extent (Garg, 1974). It was argued in Deng et al. (2015b) that the optical efficiency
 220 (effective transmittance-absorptance product) of a flat plate solar air collector was
 221 decreased by 8.39% when the transparent cover of the collector was under the condition

222 of artificially severe dust deposition. Tanesab et al. (2019) presented the effect of dust
223 with different morphologies on the performance degradation of various photovoltaic
224 technologies. Nevertheless, the aforementioned methods used to quantify the dust
225 deposition effect were limited to the case of installed solar collectors in service, as it
226 was difficult to separate the solar collectors from operating systems. On this occasion,
227 the quick measurement method provides a pathway for assessing the dust deposition
228 effect on the collector thermal performance. The transmittance-absorptance products of
229 the solar collectors in different degrees of cleanness can be obtained by quick optical
230 tests. The dust deposition effect of the solar collectors can be assessed compared to the
231 collector zero-loss optical efficiency $((\tau\alpha)_{en})$ with a clean surface.

232

233 On the other aspect, for the flat plate solar collectors serviced in solar thermal fields
234 and exposed to sunlight in the long-term running, optical performance of the collector
235 coating surfaces might be attenuated due to aging (Tian et al., 2019). It is difficult to
236 quantify the thermal performance attenuation of the installed solar collectors without
237 damaging the panels. The quick measurement method is expected to determine the
238 collector optical property attenuation after a long period of running.

239

240 **4 Conclusion**

241 A quick measurement method using a spectroradiometer was presented to identify the
242 incidence angle modifier (IAM) of flat plate solar collectors with less effort by using a
243 spectroradiometer, compared to the thermal performance test method recommended in

244 existing test standards. To testify the quick method, an installed solar photovoltaic panel
245 was used to conduct optical tests under conditions of different incidence angles. The
246 IAM coefficient of the flat solar panel was obtained with a relatively high R^2 ,
247 confirming the applicability of the quick measurement method. Last but not the least,
248 the method not only helps to determine the collector IAM quickly without needing to
249 run the collectors by energy power input, but also provides a pathway for assessing the
250 dust deposition effect and optical property attenuation of installed solar collectors in
251 the long-term running.

252

253 **Declaration of interest:** none.

254 **Acknowledgment**

255 The third author Shicong Zhang wishes to thank the support from the National Key
256 R&D Program of China (Grant No. 2017YFC0702600).

257

258 **References**

259 Aleksiejuk, J., Chochowski, A., Reshetiuk, V., 2018. Analog model of dynamics of a
260 flat-plate solar collector. *Sol. Energy* 160, 103–116.

261 <https://doi.org/10.1016/j.solener.2017.11.079>

262 ASHRAE, 2014. Standard 93-2010 (RA 2014) -- Methods of Testing to Determine the

263 Thermal Performance of Solar Collectors (ANSI Approved), ANSI/ASHRAE
264 Standard 93-2010 (R2014). ASHRAE Inc., Atlanta, USA.

265 Deng, J., Ma, R., Yuan, G., Chang, C., Yang, X., 2016. Dynamic thermal performance
266 prediction model for the flat-plate solar collectors based on the two-node lumped
267 heat capacitance method. Sol. Energy 135.
268 <https://doi.org/10.1016/j.solener.2016.06.060>

269 Deng, J., Yang, X., Wang, P., 2017. Study on the second-order transfer function models
270 for dynamic tests of flat-plate solar collectors Part II: Experimental validation. Sol.
271 Energy 141, 334–346. <https://doi.org/10.1016/j.solener.2015.01.045>

272 Deng, J., Yang, X., Wang, P., 2015a. Study on the second-order transfer function models
273 for dynamic tests of flat-plate solar collectors Part I: A proposed new model and a
274 fitting methodology. Sol. Energy 114, 418–426.
275 <https://doi.org/10.1016/j.solener.2015.01.046>

276 Deng, J., Yang, X., Yang, M., Wang, Z., 2015b. Experimental Study of a Single-pass
277 Flat Plate Solar air Collector with Severe Dust Deposition on the Transparent
278 Glass Cover. Energy Procedia 70, 32–40.
279 <https://doi.org/10.1016/j.egypro.2015.02.094>

280 Duffie, J.A., Beckman, W.A., 2013. Solar Engineering of Thermal Processes: Fourth
281 Edition, Solar Engineering of Thermal Processes: Fourth Edition.
282 <https://doi.org/10.1002/9781118671603>

283 Garg, H.P., 1974. Effect of dirt on transparent covers in flat-plate solar energy collectors
284 15, 299–302.

285 Hertel, J.D., Martinez-Moll, V., Pujol-Nadal, R., 2015. Estimation of the influence of
286 different incidence angle modifier models on the biaxial factorization approach.
287 Energy Convers. Manag. 106, 249–259.
288 <https://doi.org/10.1016/j.enconman.2015.08.082>

289 Rojas, D., Beermann, J., Klein, S.A., Reindl, D.T., 2008. Thermal performance testing
290 of flat-plate collectors. Sol. Energy 82, 746–757.
291 <https://doi.org/10.1016/j.solener.2008.02.001>

292 Sallaberry, F., Pujol-Nadal, R., De Jalón, A.G., Martínez-Moll, V., 2015. Toward a
293 standard testing methodology for solar thermal collectors with variable-geometry:
294 The direct radiation incidence angle modifier issue. Sol. Energy 121, 31–40.
295 <https://doi.org/10.1016/j.solener.2015.05.029>

296 Tanesab, J., Parlevliet, D., Whale, J., Urnee, T., 2019. The effect of dust with different
297 morphologies on the performance degradation of photovoltaic modules. Sustain.
298 Energy Technol. Assessments 31, 347–354.
299 <https://doi.org/10.1016/j.seta.2018.12.024>

300 Tesfamichael, T., Wäckelgård, E., 2000. Angular solar absorptance and incident angle
301 modifier of selective absorbers for solar thermal collectors. Sol. Energy 68, 335–
302 341. [https://doi.org/10.1016/S0038-092X\(00\)00029-3](https://doi.org/10.1016/S0038-092X(00)00029-3)

303 The British Standards Institution, 2018. BS EN ISO 9806 : 2017 Solar energy. Solar
304 thermal collectors. Test methods, British Standards. BSI Standards Limited 2018,
305 London, UK.

306 Tian, Z., Perers, B., Furbo, S., Fan, J., 2018. Analysis and validation of a quasi-dynamic

307 model for a solar collector field with flat plate collectors and parabolic trough
308 collectors in series for district heating. Energy 142, 130–138.
309 <https://doi.org/10.1016/j.energy.2017.09.135>

310 Tian, Z., Perers, B., Furbo, S., Fan, J., 2017. Annual measured and simulated thermal
311 performance analysis of a hybrid solar district heating plant with flat plate
312 collectors and parabolic trough collectors in series. Appl. Energy 205, 417–427.
313 <https://doi.org/10.1016/j.apenergy.2017.07.139>

314 Tian, Z., Zhang, S., Deng, J., Fan, J., Huang, J., Kong, W., Perers, B., Furbo, S., 2019.
315 Large-scale solar district heating plants in Danish smart thermal grid:
316 Developments and recent trends. Energy Convers. Manag. 189, 67–80.
317 <https://doi.org/10.1016/j.enconman.2019.03.071>

318

319

320

321

322

323 **Table Captions:**

324 Table 1. Comparison between the available method in the test standards and the
325 presented method

326

327 **Figure Captions:**

328 Figure 1 Testing facilities (a) fiber-optic tip of the spectrometer and reflectance standard
329 RS50; (b) solar panel in test

330 Figure 2 Measured reflectance spectrum of the tested solar panel with fiber-optic tip

331 pointing in the normal direction of the solar panel and to a vertical reference plane

332 Figure 3 Corrected reflectance spectra at different incidence angles for the solar panel

333 tested

334 Figure 4 Linear fitting of transmittance-absorptance product $(\tau\alpha)_\theta$ versus $[1/\cos\theta -$

335 $1]$ ($x = b_0 \cdot (1/\cos\theta - 1)$, $y = (\tau\alpha)_\theta$)